Frustrated Heisenberg antiferromagnets: Fluctuation-induced first order *vs.* deconfined quantum criticality

F. Krüger[1] and S. Scheidl[2]

[1] *Instituut-Lorentz, Universiteit Leiden - P.O. Box 9506*
2300 RA Leiden, The Netherlands
[2] *Institut für Theoretische Physik, Universität zu Köln*
Zülpicher Str. 77, D-50937 Köln, Germany

Abstract. – Recently it was argued that quantum phase transitions can be radically different from classical phase transitions with, as a highlight, the "deconfined critical points" exhibiting fractionalization of quantum numbers due to Berry phase effects. Such transitions are supposed to occur in frustrated ("J_1-J_2") quantum magnets. We have developed a novel renormalization approach for such systems which is fully respecting the underlying lattice structure. According to our findings, another profound phenomenon is around the corner: a fluctuation-induced (order-out-of-disorder) first-order transition. This has to occur for large spin and we conjecture that it is responsible for the weakly first-order behavior recently observed in numerical simulations for frustrated $S = 1/2$ systems.

Introduction. – Frustrated magnets exhibit quantum phase transitions of a rich variety which is the subject of intense current research [1]. Novel scenarios for phase transitions beyond the Landau-Ginzburg-Wilson (LGW) paradigm have been suggested [2,3] joggling fundamental concepts. The Heisenberg model on a square lattice with antiferromagnetic couplings J_1 and J_2 between nearest and next-nearest neighbors serves as a prototype for studying magnetic quantum-phase transitions (see, *e.g.*, [4] and references therein). From the classical limit one expects that two different magnetic orders can exist: the Néel phase with ordering wave vector (π, π) is favorable for $\alpha \equiv J_2/J_1 < 1/2$ and columnar order with $(0, \pi)$ for $\alpha > 1/2$.

Quantum fluctuations certainly may induce a paramagnetic (PM) phase which is naturally expected near $\alpha \approx 1/2$ where both orders compete [5]. Remarkably, additional orders may appear in the Néel phase as well as in the PM phase when translation symmetry is broken by an additional spin dimerization [4]. The existence of such enhanced order crucially depends on the spin value S. This becomes most apparent when the spin system is represented by a nonlinear-sigma model. Topological excitations associated with Berry phases can give rise to ground-state degeneracies corresponding to a translation-symmetry breaking by dimerization and formation of valence-bond solid (VBS) phases [6,7].

The Néel-VBS transition has been argued to be in a novel quantum criticality class that does not fit in the standard LGW paradigm. Intriguing data on this transition was obtained in simulations of the $S = 1/2$ quantum XY model frustrated by ring exchange [8, 9]. The transition was interpreted as a second-order one; this possibility was predicted by the theory of the deconfined critical point and suggested to be generic for a variety of experimentally relevant two-dimensional antiferromagnets [3]. However, in a more careful finite-size analysis of the XY case it was demonstrated that the Néel-VBS point represents an anomalously weak first-order transition [10].

Field-theoretical approaches of various kinds have been developed, based on the $1/S$ [11] or the $1/N$ expansion [12,13]. The latter approach is able to capture some of the essence of the topological aspects on a mean-field level. However, it is the former approach, elaborated to a renormalization-group analysis, which predominantly has served as basis for a comparison of critical aspects between theory and experiment (see, *e.g.*, [14]).

Nevertheless, this approach so far has suffered from two intrinsic shortcomings: i) Spin-wave interactions are the physical mechanism underlying the renormalization flow. On one-loop level, the flow equations describe corrections to the physical parameters of relative order $1/S$. These corrections have been worked out using a continuum version of the nonlinear σ model (CNLσM) as a starting point [11]. However, for the original lattice model, this is not systematic, since corrections of the same order are dropped under the naive coarse graining of the lattice model onto the CNLσM. As a consequence, important effects such as a renormalization of the spin-wave velocity and the frustration α are missed. ii) Similarly, the outer large momentum region of the magnetic Brillouin zone (BZ) is only crudely treated. This entails a significant uncertainty in the computation of the phase diagram.

In this letter, we lift these shortcomings by developing a renormalization analysis which fully accounts for the lattice structure. It combines the systematic treatment of all corrections in order $1/S$ on the level of the conventional first-order spin-wave theory (SWT) with the merits of a renormalization approach, which goes beyond any finite order in $1/S$ by an infinite iteration of differential steps, successively eliminating the spin-wave modes of highest energy. As a result, we obtain an improved description of the phase transitions. In particular, the possibility of a fluctuation-induced first-order transition which is not accessible on the level of the CNLσM is included in a natural way.

Spin-coherent state representation. –   The key to what follows is a novel kind of path integral quantization, which makes it possible for us to treat the effects of umklapp on an equal footing with the spin-wave interactions. To be specific, we stick to the aforementioned J_1-J_2 Heisenberg model on a square lattice. We address the stability of the Néel phase against quantum fluctuations controlled by S and α. Fluctuations are treated in a coherent spin state path-integral representation of the model, where a spin state corresponds to a unit vector $\vec{n}$. In the absence of fluctuations, spins would assume the states $|\vec{n}_{A/B}\rangle = |\pm\vec{e}_z\rangle = |S, \pm S\rangle$ on the two sublattices A and B. From the standard Trotter formula there emerge an imaginary time τ (discretized in intervals of duration $\Delta\tau$) and an action of the form [1]

$$\mathcal{S} = -\sum_\tau \ln\langle\{\vec{n}\}|\{\vec{n}'\}\rangle + \sum_\tau \Delta\tau \frac{\langle\{\vec{n}\}|\hat{H}|\{\vec{n}'\}\rangle}{\langle\{\vec{n}\}|\{\vec{n}'\}\rangle} \tag{1}$$

taking $\vec{n}$ at time τ and $\vec{n}'$ at $\tau - \Delta\tau$. For weak quantum fluctuations, the components of $n_{x,y}$ perpendicular to the magnetization axis are small and may be considered as expansion parameters (as in [11]). However, attempting to directly apply this expansion to the lattice model we encountered time ordering difficulties in the action [15].

Instead, we start form a stereographic parametrization of coherent states, on sublattice A, $|\vec{n}\rangle = (1 + \bar{a}a/2S)^{-S} \exp[a\hat{S}_-/\sqrt{2S}])|S, S\rangle$, where a is the stereographic projection of $\vec{n}$ from the unit sphere onto the complex plane, $a = \tan(\theta/2)\exp[i\phi]$ with the standard spherical angles θ and ϕ. The action can be expressed in terms of the stereographic coordinates using the matrix elements [16]

$$\frac{\langle\vec{n}|\hat{S}_z|\vec{n}'\rangle}{\langle\vec{n}|\vec{n}'\rangle} = S\frac{1 - \bar{a}a'/2S}{1 + \bar{a}a'/2S}, \quad \frac{\langle\vec{n}|\hat{S}_+|\vec{n}'\rangle}{\langle\vec{n}|\vec{n}'\rangle} = \frac{\sqrt{2S}\,a'}{1 + \bar{a}a'/2S}. \tag{2}$$

Here $\bar{a}$ is the complex conjugate of a. The expressions for the coordinate b on sublattice B are given by the correspondences $\hat{S}_z \rightarrow -\hat{S}_z$ and $\hat{S}_\pm \equiv \hat{S}_x \pm \hat{S}_y \rightarrow \hat{S}_\mp$ for $a \rightarrow b$.

The explicit expression of the action in terms of a and b is too lengthy to be given here. To leading order in $1/S$, the fluctuations are controlled by the bilinear part $\mathcal{S}_0$ of the action that represents free magnons. We also retain the quartic contribution $\mathcal{S}_{\text{int}}$ to the action, which represents magnon interactions and contains the renormalization of single-magnon parameters of relative order $1/S$. Higher-order contributions to the action are neglected. Terms from the functional Jacobian are also negligible on this level. The single-magnon contribution to the action can be parameterized in the form

$$\mathcal{S}_0 = \sum_\tau \int_{\boldsymbol{k}} \left\{ \frac{1}{2g}[\bar{a}_{\boldsymbol{k}}\Delta a_{\boldsymbol{k}} - \Delta\bar{a}_{\boldsymbol{k}}a'_{\boldsymbol{k}} + \bar{b}_{\boldsymbol{k}}\Delta b_{\boldsymbol{k}} - \Delta\bar{b}_{\boldsymbol{k}}b'_{\boldsymbol{k}}] + \right.$$
$$\left. + \Delta\tau S[\Gamma^+_{\boldsymbol{k}}(\bar{a}_{\boldsymbol{k}}a'_{\boldsymbol{k}} + \bar{b}_{\boldsymbol{k}}b'_{\boldsymbol{k}}) + \Gamma^-_{\boldsymbol{k}}(\bar{a}_{\boldsymbol{k}}\bar{b}_{\boldsymbol{k}} + a'_{\boldsymbol{k}}b'_{\boldsymbol{k}})] \right\}, \tag{3}$$

using the Fourier transform $a(\boldsymbol{r}) = \int_{\boldsymbol{k}} e^{i\boldsymbol{k}\cdot\boldsymbol{r}}a_{\boldsymbol{k}}$, the integral $\int_{\boldsymbol{k}} = 2\int \frac{\mathrm{d}^2k}{(2\pi)^2}$ over the magnetic BZ $|k_x| + |k_y| \leq \pi$, and the exchange couplings $\Gamma^+_{\boldsymbol{k}} \equiv J^+_{\boldsymbol{k}} - J^+_0 + J^-_0$, $\Gamma^-_{\boldsymbol{k}} \equiv J^-_{\boldsymbol{k}} \equiv 2J_1[\cos(k_x) + \cos(k_y)]$ and $J^+_{\boldsymbol{k}} = 2J_2[\cos(k_x + k_y) + \cos(k_x - k_y)]$. For simplicity, the lattice constant is considered as unit length. The dimensionless parameter g represents the strength of quantum fluctuations. It assumes the value $g = 1$ in the unrenormalized model and turns out to increase under renormalization.

Diagonalizing this bilinear action, one easily obtains the magnon dispersion $E_{\boldsymbol{k}} = Sg|\Gamma^+_{\boldsymbol{k}}|\sqrt{1 - \gamma^2_{\boldsymbol{k}}}$, where $\gamma_{\boldsymbol{k}} = \Gamma^-_{\boldsymbol{k}}/\Gamma^+_{\boldsymbol{k}}$. For $\alpha \leq 1/2$, the low-energy spin-wave excitations are characterized by an isotropic dispersion $E(\boldsymbol{k}) = c|\boldsymbol{k}| + \mathrm{O}(k^2)$ with a spin-wave velocity $c = \sqrt{8g}SJ_1\sqrt{1 - 2\alpha}$. Likewise, the exchange couplings generate a spin stiffness $\rho = S^2J_1(1 - 2\alpha)$ for low-energy modes. One also obtains the propagators $\langle\bar{\phi}_{\boldsymbol{k}}\phi'_{\boldsymbol{k}}\rangle = gG_{\boldsymbol{k}}$ and $\langle\bar{\phi}_{\boldsymbol{k}}\phi_{\boldsymbol{k}}\rangle = \langle\bar{\phi}'_{\boldsymbol{k}}\phi_{\boldsymbol{k}}\rangle = g(G_{\boldsymbol{k}} + 1)$ for fields from the same sublattice ($\phi = a, b$), and $\langle a_{\boldsymbol{k}}b_{\boldsymbol{k}}\rangle = \langle\bar{a}_{\boldsymbol{k}}\bar{b}_{\boldsymbol{k}}\rangle = -gF_{\boldsymbol{k}}$ for fields from different sublattices. In the latter case the correlators are unchanged by a replacement $\bar{\phi} \rightarrow \bar{\phi}'$. We have defined $G_{\boldsymbol{k}} = (n_{\boldsymbol{k}} + 1/2)(1 - \gamma^2_{\boldsymbol{k}})^{-1/2} - 1/2$ and $F_{\boldsymbol{k}} = (n_{\boldsymbol{k}} + 1/2)\gamma_{\boldsymbol{k}}(1 - \gamma^2_{\boldsymbol{k}})^{-1/2}$ where $n_{\boldsymbol{k}} = (e^{\beta E_{\boldsymbol{k}}} - 1)^{-1}$ is the bosonic occupation number. For strong frustration ($\alpha > 1/2$) the stiffness becomes negative and the spin-wave velocity is ill-defined due to the presence of unstable modes in the center of the BZ (see fig. 1).

Renormalization approach. – Starting from this action with bilinear and quartic terms, we implement a renormalization procedure as follows. In successive steps, the modes of highest energy (an infinitesimal fraction of all modes) are integrated out. This decimation of modes yields an effective theory for the remaining modes and gives rise to differential flow equations. As flow parameter we choose $l = \frac{1}{2}\ln(A_{\text{BZ}}/A_{\text{RBZ}})$, where $A_{\text{BZ}} = 2\pi^2$ is the area of the original BZ, and A_{RBZ} is the area of the residual BZ (RBZ) populated by the remaining modes. On large length scales in the Néel phase, the RBZ becomes circular and l is the usual logarithmic
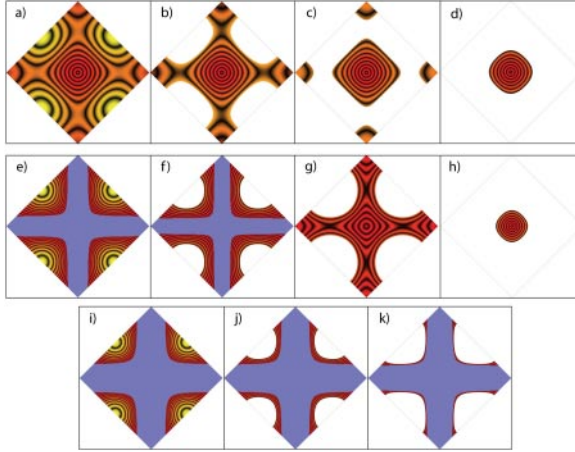
Fig. 1 – (Color on-line) Evolution of modes under coarse graining. Each panel corresponds to the area $|k_x| \leq \pi$, $|k_y| \leq \pi$. Red color represents small, yellow high positive energy. Black lines are lines of constant energy, blue areas represent unstable modes. Panels (a)-(d): in the Néel phase the RBZ may become disconnected first, then always shrinks to a sphere (here $S = 1/2$, $\alpha = 0.3$, $l = 0, 0.25, 0.5, 1.0$). Panels (e)-(h): in the Néel phase for strong frustration $\alpha > 1/2$, initially unstable modes (blue area) are renormalized to stable modes and the RBZ eventually also shrinks to a sphere (here $S = 1/2$, $\alpha = 0.55$, $l = 0, 0.11, 0.29, 1.30$). Panels (i)-(k): in the columnar phase, after the elimination of all stable modes, an area of unstable modes survives (here $S = 2$, $\alpha = 0.6$, $l = 0, 0.10, 0.20$).

length scale. The evolution of the RBZ and the single-magnon dispersion is illustrated in fig. 1 for various parameters.

To one-loop order, corresponding to a systematical calculation of corrections in order $1/S$, the renormalization effects due to spin-wave interactions can be captured by a flow of the single-magnon parameters. The resulting flow equations are given by

$$\mathrm{d}g^{-1} = -\frac{1}{S}\mathrm{d}G^0, \tag{4}$$

$$\mathrm{d}J_1 = \frac{g}{S}J_1(\mathrm{d}F^- - 2\mathrm{d}G^0), \tag{5}$$

$$\mathrm{d}J_2 = \frac{g}{S}J_2(\mathrm{d}G^+ - 2\mathrm{d}G^0), \tag{6}$$

where the integrals over the differential fraction ∂ of modes of highest energy are defined as $\mathrm{d}G^0 = \int_{\boldsymbol{q}}^{\partial} G_{\boldsymbol{q}}$, $\mathrm{d}G^+ = \int_{\boldsymbol{q}}^{\partial}(J_{\boldsymbol{q}}^+/J_0^+)G_{\boldsymbol{q}}$, and $\mathrm{d}F^- = \int_{\boldsymbol{q}}^{\partial}(J_{\boldsymbol{q}}^-/J_0^-)F_{\boldsymbol{q}}$.

Since the BZ does not remain self-similar under mode decimation, we omit the usual rescaling of length and time which is necessary only for the identification of fixed points under a renormalization-group flow. However, dropping this rescaling does not lead to a loss of information. Then, each fixed point represents an antiferromagnetically ordered state. The quantum-disordered phase and the transition into it show up as run-away flow.

Results and discussion. –   Because of the changing geometry of the RBZ and the incorporation of the full single-magnon dispersion in our renormalization approach, the flow equations can be integrated only numerically. Here, we focus on $T = 0$, although the flow equations are valid also for $T > 0$. The flow of parameters is characterized by the following tendencies. Both exchange couplings $J_{1,2}$ as well as $1/g$ always shrink. These fundamental parameters
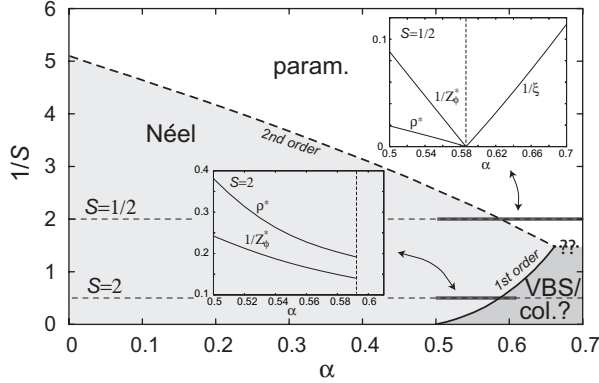
Fig. 2 – Phase diagram showing the 2nd-order transition line between the Néel ordered and the PM phase (dashed line) and the 1st-order boundary between the Néel and the columnar phase (solid line). The border between the PM and the columnar phase (dotted line) is just guesswork and cannot be calculated within our approach. Insets: nature of the phase transitions. For $S = 1/2$ the renormalized spin stiffness ρ^* vanishes and the strength of the quantum fluctuations Z_ϕ^* diverges at the phase boundary corresponding to a 2nd-order transition. Close to the the Néel phase the correlation length diverges like $\xi \sim (\alpha - \alpha_c)^{-1}$. At the 1st-order transition ($S = 2$) ρ^* and Z_ϕ^* remain finite.

flow in such a way that α always decreases, c^2 increases (initially it is negative for $\alpha > 1/2$), while ρ may increase for small l until it decreases for sufficiently large l.

The nature of magnetic order can be identified from the flow behavior. Three possibilities are observed. i) The RBZ shrinks to a circle of decreasing radius $\propto e^{-l}$ (see fig. 1 panels (a)-(d) and panels (e)-(h)) while $J_{1,2}$ and g (as well as the derived quantities c, ρ, α) converge to positive values. In this asymptotic large-scale limit our flow equations match perfectly with those derived from a CNLσM [11]. Then Néel order is present, characterized by these renormalized low-energy parameters. ii) At some finite l^*, fluctuations become so strong that g diverges and $J_{1,2}$ vanish. This indicates the loss of magnetic order due to overwhelming quantum fluctuations. Close to the transition to the Néel phase, the magnetic correlation length —which can be identified with $\xi = e^{l^*}$— diverges algebraically like $\xi \sim (\alpha - \alpha_c)^{-1}$. For $S = 1/2$ this asymptotic behavior is shown in one inset of fig. 2. iii) For strong frustration, it is also possible that a finite RBZ of unstable modes remains after decimation of *all* stable modes (see fig. 1 panels (i)-(k)). This indicates that the instability towards columnar order is effective for the renormalized low-energy modes.

The region of stability of the Néel phase is illustrated by the light-grey region in fig. 2. In the absence of frustration, we find Néel order to be stable for $1/S \lesssim 5.09$ in remarkable agreement with conventional linear SWT [5]. However, this is pure coincidence since in linear SWT the phase boundary is determined by the vanishing of the local magnetization calculated in order S^0, whereas here it is determined by the divergence of g due to spin-wave interactions treated in one-loop order. While the phase boundary is located at academically small spin values for small frustration, S reaches physically meaningful values at larger frustration where the discrepancies between SWT and our renormalization approach become more pronounced. In linear SWT, the phase boundary smoothly approaches $1/S \searrow 0$ for $\alpha \nearrow 0.5$, whereas we find the Néel phase to reach up to $\alpha = 0.66$ for $S = 0.68$. For spins smaller than this value, the Néel phase becomes unstable towards a PM phase via a second-order transition, whereas it becomes unstable for $S > 0.68$ via a first-order transition. Since we deal with a discontinuous
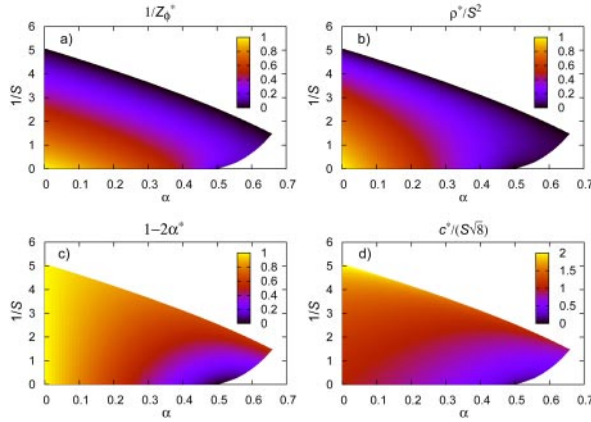
Fig. 3 – (Color on-line) Values of the renormalized parameters within the Néel phase. Color corresponds to the strength of large-scale fluctuations (a), the renormalized spin stiffness (b), the frustration (c), and the spin-wave velocity (d).

transition we can only speculate about the type of ordering in the adjacent phase (dark-shaded region in fig. 2). From the classical limit we expect columnar order for very large S whereas for intermediate spin also VBS order may be present.

In the region where the Néel phase reaches up to $\alpha > 1/2$, initially unstable modes are renormalized to stable ones by spin-wave interactions. Simultaneously, α is renormalized to a value $\alpha^* < 1/2$ and the flow behavior i) is realized. In the columnar phase, the flow of α saturates at a value $\alpha^* > 1/2$ and the flow behavior iii) is observed.

Stability of Néel order for $\alpha > 0.5$ so far has been found only by a self-consistently modified SWT [17] and Schwinger-boson mean-field theory (SBMFT) [18]. The overall shape of the Néel phase of these approaches is consistent with our findings. However, the first-order line has a more pronounced curvature in our theory and the Néel phase extends less in the $\alpha > 1/2$ region. Whereas in modified SWT and SBMFT the first-order transition from Néel to columnar order is obtained by a comparison of free energies between the two phases in our theory, an instability towards a fluctuation-induced first-order transition directly emerges from the analysis of spin-wave interactions in the Néel phase without any assumptions about the order in the adjacent phase. Of course, for intermediate spin VBS phases may have a lower energy than the columnar phase.

The nature of the transitions out of the Néel phase becomes apparent from the behavior of the fluctuations on large length scales ($k \to 0$), where $\langle \bar{\phi}_{\boldsymbol{k}} \phi'_{\boldsymbol{k}} \rangle \simeq \frac{Z_\phi}{\sqrt{2}k}$ with $Z_\phi \equiv \frac{g}{\sqrt{1-2\alpha}} \propto \frac{c}{\rho}$. Approaching the transition into the PM phase, the renormalized value Z_ϕ^* diverges and gives rise to a divergent susceptibility (see fig. 3). At the same time the renormalized ρ^* vanishes while c^* remains finite. The continuous evolution of Z_ϕ^* and ρ^* indicates the second-order nature of the transition. Approaching the transition into the columnar phase, one observes a saturation of Z_ϕ^* and ρ^* at finite values as well as a discontinuous jump of α^* indicating a first-order transition. Figure 3 illustrates the dependence of various renormalized quantities on α and $1/S$ within the Néel phase. The insets of fig. 2 show the evolution of ρ^*, Z_ϕ^* and ξ with higher resolution at the transitions.

Confidence in the reliability of our findings is provided by quantitative comparisons for specific parameter values. Results for $Z_c^* \equiv c^*/c$ exist from various approaches. For $S = 1/2$ and

$\alpha = 0$, first-order SWT yields a slight enhancement of spin-wave velocity, $Z_c^{\text{SWT}} = 1.158$. We find an increased value $Z_c^* = 1.20$, which is in agreement with Monte Carlo (MC) simulations (see [19] and references therein). As $1/S$ and/or α increases, the enhancement factor Z_c^* also increases. At the phase boundary $1/S \approx 5.09$ for $\alpha = 0$, the difference is already more pronounced: $Z_c^{\text{SWT}} = 1.40$ and $Z_c^* = 2.04$. For $\alpha > 0$, unfortunately, MC data for Z_c are not available at the transition out of the Néel phase, either for $S = 1/2$ or for larger physical values of S.

Conclusion. – We have presented a novel renormalization approach for frustrated quantum antiferromagnets which fully accounts for the underlying lattice geometry and consistently captures the renormalization of the single-magnon parameters by spin-wave interactions all over the magnetic BZ.

For the J_1-J_2 model we clearly demonstrated that for large spins and strong frustration, fluctuations on lattice and intermediate scales cause an instability of the Néel phase towards a first-order transition. These effects are totally missed by any effective long-wavelength continuum theory obtained by a naive coarse graining of the lattice model.

We conjecture that these fluctuations which crucially depend on the underlying lattice geometry and the way of frustrating the Néel order are responsible for the weakly first-order behavior observed recently in numerical simulations for frustrated $S = 1/2$ systems [10].

$$* * *$$

REFERENCES

[1] Sachdev S., *Quantum Phase Transitions* (Cambridge University Press, Cambridge, England) 1999.
[2] Senthil T., Balents L., Sachdev S., Vishwanath A. and Fisher M. P. A., *Phys. Rev. B*, **70** (2004) 144407.
[3] Senthil T., Vishwanath A., Balents L., Sachdev S. and Fisher M. P. A., *Science*, **303** (2004) 1490.
[4] Sushkov O. P., Oitmaa J. and Weihong Z., *Phys. Rev. B*, **63** (2001) 104420.
[5] Chandra P. and Doucot B., *Phys. Rev. B*, **38** (1988) R9335.
[6] Haldane F. D. M., *Phys. Rev. Lett.*, **61** (1988) 1029.
[7] Fradkin E. and Stone M., *Phys. Rev. B*, **38** (1988) R7215.
[8] Sandvik A. W., Daul S., Singh R. R. P. and Scalapino D. J., *Phys. Rev. Lett.*, **89** (2002) 247201.
[9] Melko R. G., Sandvik A. W. and Scalapino D. J., *Phys. Rev. B*, **38** (2004) R9335.
[10] Kuklov A., Prokof'ev N. and Svistunov B., *Phys. Rev. Lett.*, **93** (2004) 230402.
[11] Chakravarty S., Halperin B. and Nelson D. R., *Phys. Rev. B*, **39** (1989) 2344.
[12] Read N. and Sachdev S., *Phys. Rev. Lett.*, **62** (1989) 1694.
[13] Read N. and Sachdev S., *Phys. Rev. B*, **42** (1990) 4568.
[14] Hasenfratz P., *Eur. Phys. J. B*, **13** (2000) 11.
[15] Krüger F. and Scheidl S., unpublished.
[16] Radcliffe J. M., *J. Phys. A*, **4** (1971) 313.
[17] Xu J. H. and Ting C. S., *Phys. Rev. B*, **42** (1990) R6861.
[18] Mila F., Poilblanc D. and Bruder C., *Phys. Rev. B*, **43** (1991) 7891.
[19] Manousakis E., *Rev. Mod. Phys.*, **63** (1991) 1.